3D printable geomaterials

D. a H Hanaor, Y. Gan, M. Revay, D. W Airey, I. Einav

Hanaor, D. A. H., Gan, Y., Revay, M., Airey, D. W., & Einav, I. (2016). 3D printable geomaterials. *Géotechnique*, *66*(4), 323-332.

3D Printable Geomaterials

D.A.H. Hanaor, Y. Gan, M. Revay, D. Airey, I. Einav

School of Civil Engineering, University of Sydney, NSW 2006, Australia

Abstract

One of the many attributes of 3D printing is the ability to produce particles with independent control of morphology and material properties, parameters that are inexorably entwined in naturally occurring geomaterials. In this paper we describe the 3D printing of surrogate granular materials, show examples of the particles produced and present results showing their ability to capture real soil behaviour. Three approaches are demonstrated for the three dimensional generation of model grains. The first method involves the superimposition of a fractal surface with higher level stochastic features on the face of a closed volume such as a geodesic spheroid. The second method involves the use of Fourier descriptors or fractal geometry generated from 2D cross sections and their interpolation to produce simulated geomaterial particles in three dimensions. The third method involves the generation of complex particles by the aggregation of polyhedral elements such as cubes or octahedra which is suitable for the simulation and fabrication of porous or branching particles. Finally, we discuss applications of the fabrication of surrogate materials by 3D printing for use as standardised, printable geomaterials in future up-scaled geotechnical experiments and other geomechanical research.

Keywords: Granular media; 3D morphology; Shape generation; Surfaces

*Corresponding Author- email: itai.einav@sydney.edu.au; Ph +61-2-9351-2069

1. Introduction

Understanding the micromechanical origins of the behaviour of granular materials is of increasing interest across multiple disciplines in science and engineering. In a broad range of naturally occurring granular materials, including soils, sediment particles, sand rocks and minerals, there is a need to establish better relationships between the multi-scale particle morphology of these geomaterials and their mechanical, hydrological, and rheological performance. This has the potential to enable more efficient utilisation of natural resources and improved reliability in geotechnical and environmental applications (Scheel et al., 2008, Salot et al., 2009). Recent years have seen increasing research efforts aimed at gaining new insights into such relationships through computational and experimental methods (Brisard et al., 2012, Cho et al., 2006, Cavarretta et al., 2010, Mollon and Zhao, 2013b).

The utility and significance of 3D printing techniques for the analysis of granular morphology was demonstrated recently in a study by Miskin and Jaeger (Miskin and Jaeger, 2013). In this study idealised printed grains were constructed by joining 1 to 4 spherical units with minimum overlaps between the spheres. The growth in the capabilities and reducing cost of 3D printing technologies, combined with the availability of computational resources that permit high resolution, have made it possible to produce grain morphologies representative of real geomaterial particles in large quantities. Furthermore, the range of materials has expanded, facilitating the fabrication of complex grains with fixed morphology for different material properties. These capabilities now allow independent control of morphology and material properties.

The simulation of realistic geomaterial grain morphologies is of value, not only in 3D printing but also for discrete element method (DEM) models of granular materials (Matsushima et al., 2014). Such methods have often assumed simplified geometries such as spherical or circular elements (Persson and Frenning, 2012, Cundall et al., 1979), clustered spheres or disks (Thomas and Bray, 1999), polygons (Alonso-Marroquín et al., 2008) or sphero-polygons (Alonso-Marroquin, 2008, Alonso-Marroquín and Wang, 2009) and polyhedra (Langston et al., 2013). While these simplified geometries may be utilised effectively on a case by case basis, the hierarchical origins of surface-localised physical behaviour in geomaterials means that more complex approaches are necessary for the purposes of describing, predicting or explaining the morphological dependence of these characteristics (Alonso-Marroquín et al., 2013, Hanaor et al., 2013).

In naturally occurring geomaterials macroscopically observed properties of friction and contact stiffness between grains are, in addition to bulk properties, governed by surface structures, which exhibit self-affine geometries showing features across a range of length-scales (Russel, 2014, Hanaor et al., 2014). One can consider surface structures of granular material as an extension of hierarchical morphology exhibiting non-integer dimensionality (Arasan et al., 2011, Qin et al., 2013). Additionally, cohesion and capillary forces between grains are also governed by surface structures (Fraysse et al., 1999), further motivating the development of methods to characterise and model natural grain morphologies.

Methods to describe and classify the morphologies of naturally occurring grains predominantly invoke measures of sphericity, roundness, convexity and roughness. These parameters have been defined in a variety of manners, and have been the subject of multiple reviews (Blott and Pye, 2008, Barrett, 1980, Pourghahramani and Forssberg, 2005). Charts put forward by Krumbein and Sloss have frequently been employed for the conventional classification of geomaterials over the past six decades (Krumbein and Sloss, 1951). However, the use of these morphological descriptors is driven primarily by convenience rather than physical meaning. Geomaterial grains are not uniquely defined by this type of descriptor and while these parameters can be extracted from image analysis with ever increasing ease (Altuhafi et al., 2012, Liao et al., 2010), they are insufficient for the computational generation and printing of simulated geomaterial particles.

Recent years have seen a growing interest in utilising Fourier descriptors to characterise particle shape on the basis of planar grain projections. This approach was first put forward in 1970 (Ehrlich and Weinberg, 1970) and utilises the Fourier spectrum of 2D contours to characterise grain morphology in terms of a series of numerical

descriptors (Bowman et al., 2001, Thomas et al., 1995). The notable advantage to the use of Fourier descriptors is their applicability in grain simulation procedures as pioneered by Mollon and Zhao over recent years (Mollon and Zhao, 2012, Mollon and Zhao, 2013a).

The ability to print surrogate granular material offers new research methods that can assist in establishing the micromechanical origins, and the role of morphology and material properties, on the behaviour of granular materials. Importantly, the concept of printable granular geomaterials offers an avenue to "standardise" soil for quality control and calibration in geotechnical testing. Currently standard materials in geotechnical laboratories are mineral sands and soils from particular geological sources, e.g. Ottawa sands (Tarnawski et al., 2009). This limitation could be overcome if the ability to fabricate uniform and consistent geomaterial specimens with controlled standardised properties can be attained.

In order to realise the opportunities afforded by 3D printing techniques in the study of granular materials, two identifiable criteria must be met: (i) simulated granular matter must be meaningful and realistic representations of the materials of interest; and (ii) parameters utilised in the generation of simulated granular matter should be readily acquirable from real materials.

In this paper we present and discuss methods for the three dimensional simulation of realistic granular materials for application in 3D printing of standardised surrogate geomaterials, and show examples of the 3D printed particles produced. We further present results showing the ability of a bulk quantity of the printable material to capture real sand behaviour under drained triaxial loading conditions, and examine issues relating to the utilisation of these methods in the study of micromechanical interactions in granular materials.

2. Materials and methodology:

For the different approaches presently reported, simulated grains were generated in a Matlab environment and, with all methods, individual grains were described by discrete sets of corresponding vertices and faces. Additionally, subsequent to scaling, single grains or sets of multiple grains were converted into a Standard Tessellation Language (STL) format suitable for visualisation by computed aided design (CAD) software and for fabrication by 3D printing methods. Using these methods, grains can be generated in alternative computational environments and alternate output formats can be used. Fabrication of the grains reported here was carried out using layer by layer photo-polymerisation by means of an Objet Eden 250 poly-jet type 3D printer with a spatial resolution of 32μm using Fullcure 720 resin (Stratasys, USA) in a layer by layer printing method. The cured polymer has a specific gravity of 1.19 and an elastic modulus of approximately 2 GPa.

2.1. Method 1. Fractal Surface Overlay (FSO)

Natural materials tend to exhibit multi-scale surface structures featuring statistical self-similarity or fractality. For interfaces this fractality is quantified by reference to macroscopically flat surfaces. The same approach can be applied to define the morphology of grains by their interface structure across multiple scales overlaid on a spheroidal or polygonal macrostructure.

The Ausloos-Berman type variants of the Weierstrass Mandelbrot function are used for the generation of fractal surfaces with stochastic highest level features. In macroscopically flat surfaces this can be used for the simulation of realistic surfaces. In such macroscopically planar surfaces the surface height function can be described in polar coordinates (ρ,θ) in the following form (Yan and Komvopoulos, 1998, Ausloos and Berman, 1985, Komvopoulos, 2008, Ciavarella et al., 2008, Hanaor et al., 2015)

$$Z(\rho,\theta)=\sqrt{\frac{\ln\gamma}{M}}\sum_{m=1}^{M}\sum_{n=0}^{n\max}\left(\frac{2\pi\gamma^{n}}{L}\right)^{(D-3)}\left\{\cos\psi_{m,n}-\cos\left[\frac{2\pi\gamma^{n}}{L}\rho\cos\left(\theta-\alpha_{m}\right)+\psi_{m,n}\right]\right\} \quad (1)$$

Here n corresponds to consecutive frequency exponents and, as with previous work, in this approach M and n_{max} define the number of superimposed ridges and frequencies used to construct the surface and it was found that a value of $M = n_{max} = 40$ gives a sufficiently random surface structure, such that parallel ridge networks are absent as observed in the present and prior work (Hanaor et al., 2013). γ corresponds to a scaling factor relating to the density of frequencies used to construct the surface and is set at 1.5 similar to previous work (Ciavarella et al., 2006, Yan and Komvopoulos, 1998), α_m is an arbitrary angle used to offset asperity ridges in the azimuthal direction, D is the fractal dimension, and L is a stochastic length parameter.

In applying this method to the simulation of grain surfaces, varying the stochastic length parameter L, at lower values allows for the control of the nodularity, the number of highest scale nodes protruding from the grain, or at higher values (L>πr) allows for the control of grain elongation simulated, using a variant of Eq. 1. To implement this, a geodesic sphere is simulated at a desired resolution on the basis of an icosahedral primitive unit to yield evenly distributed (θ,ϕ) pairs where θ [0 2π] is the coordinate azimuth and ϕ [0 π] is the elevation. The vectors representing the surface coordinates are adjusted to give a fractal surface structure overlaid on the geodesic sphere. This is done separately for the two hemispheres to avoid symmetry about the equator. For vertices in the first hemisphere, having $\phi \leq \pi/2$, sphere radii are adjusted in the following form

$$R_1(\theta,\varphi)=R_0+K\sum_{m=1}^{M}\sum_{n=1}^{n\max}\left(\frac{2\pi\gamma^{n-1}}{L}\right)^{(D-3)}\left\{\cos\left(\psi_{m,n}+\zeta_{m,n}\cos\varphi\right)-\cos\left[\frac{2\pi\varphi\gamma^{n}}{L}\cos\left(\theta-\alpha_{m}\right)+\psi_{m,n}+\zeta_{m,n}\cos\varphi\right]\right\} \quad (2)$$

where R_0 is the radius of the initial geodesic spheroid, ψ is a random phase angle and K is an amplitude scaling parameter. For coordinates in the second hemisphere, having values of $\phi > \pi/2$, radii are adjusted as follows

$$R_2(\theta,\varphi)=R_0+K\sum_{m=1}^{M}\sum_{n=1}^{n\max}\left(\frac{2\pi\gamma^{n-1}}{L}\right)^{(D-3)}\left\{\cos\psi_{m,n}-\cos\left[\frac{2\pi(\pi-\varphi)\gamma^{n}}{L}\cos\left(\theta-\alpha_{m}\right)+\psi_{m,n}\right]\right\} \quad (3)$$

To impart surface structure randomness, a set of randomised phase angles ψ of the size $M \times n_{max}$ is included, given by a uniform distribution $\psi_{m,n}=U(0,2\pi)$. To avoid symmetry, for the surface of the lower hemisphere where $\phi \leq \pi/2$, a second phase angle ζ is included and multiplied by the term $\cos\phi$ to give continuity of the surface across the equator (where $\phi = \pi/2$). A scaling factor K is included in order to normalise the amplitude of the surface features to a desired level relative to the initial geodesic spheroid radius R_0.

The results of this grain generation method and the effects of varying the stochastic length parameter are shown in Figure 1. By varying the proportional size of L relative to the grain radius, it is possible to create grains with a varying number of highest level features which can yield oblong, nodular or rough grain morphologies as shown. It can be seen that low L/R values tend to yield unrealistic grains exhibiting a large number of protrusions.

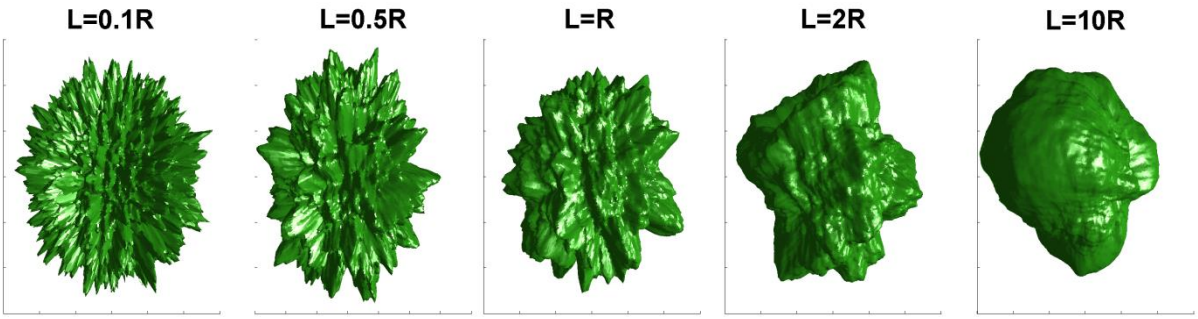

Figure 1. Grains simulated using the FSO method with the stochastic length parameter (L) varied relative to grain radius from 0.1R to 10R. Fractal Dimension is maintained constant at 2.4.

For a given value of *L/R*, the fractal dimension *D* can be varied to yield controlled surface-structure scaling behaviour illustrated in Figure 2. As with the stochastic length parameter excessively high or low fractality values leads to unrealistic grain structures in the simulated geomaterials.

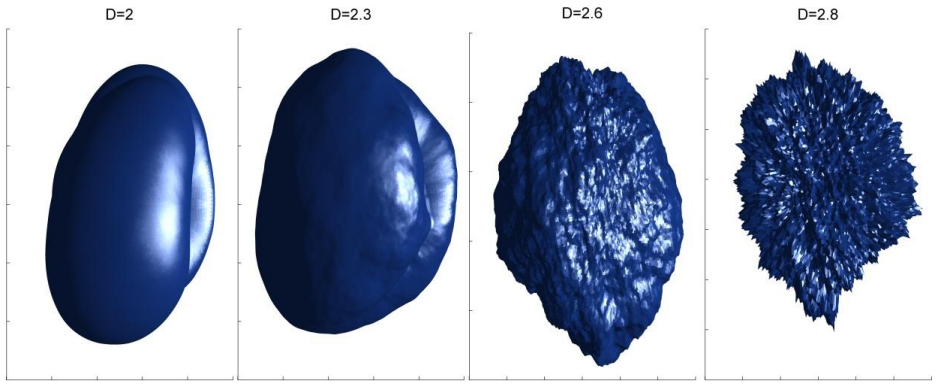

Figure 2. Grains simulated using the FSO method with the applied fractal dimension (D) varied from 2 to 2.8. Stochastic length parameter is constant at L=7R.

In the present work the precursor shape from which grains are created is a geodesic sphere. However, equivalent methodologies can be implemented using geodesic precursors generated by 3D Voronoi tessellation or other methods similar to previously reported approaches (Mollon and Zhao, 2012, Mollon and Zhao, 2014, Pena et al., 2007). By adjusting the magnitude of the barycentric vectors of the primitive geodesic object, particle morphologies are created such that all rays emanating from a definable central point within the particle intersect the particle surface exactly once. Such morphologies are also referred to as star-like (Robertson, 1936, Natalini et al., 2008). Owing to the complexity in fractal surface analysis of granular materials, with this method there are difficulties in simulating grains on the basis of parameters extracted from real geomaterials.

2.2. Method 2. Contour rotation interpolation (CRI)

The morphological characterisation of granular materials using image processing based methods, with initial data acquired through electron microscopy or optical methods, frequently yields 2-dimensional grain contours or polyhedra as output. These geometries describe planar projections of grains, as described by Cartesian or polar coordinates. Additionally, the computational simulation of geomaterial morphology is often conducted towards

the generation of such 2D geometries owing to the greater speed with which such algorithms can be implemented relative to 3D grain generation.

A novel computational method for generating realistic 3D grain morphologies on the basis of the interpolation of three 2D grain contours was first developed and reported in a recent publication by Mollon and Zhao and has been described in greater detail elsewhere (Mollon and Zhao, 2012, Mollon and Zhao, 2013a, Mollon and Zhao, 2014). Generating particles by CRI relies in principal on the generation of three closed grain cross sections, like those shown in Figure 3, followed by processes of contour correction, revolution, stretching and morphing in order to render a morphology that amalgamates the three grain projections into a single 3D object. A variety of methods can be used to obtain realistic grain sections. In Figure 3 we show examples generated by a fractal surface profile, Fourier descriptors and from a sand grain micrograph.

This method generates 3D geometries where each surface point is defined by a distinct coordinate (ρ,θ,φ). Thus, as with grain generation by FSO, this method yields starlike objects and does not allow for the generation of branching or porous morphologies.

On the basis of Mollon and Zhao's methods, contours can be generated by means of a Fourier construction, with the modes of the amplitude spectrum, known as Fourier Descriptors (FDs). Fourier descriptors 2,3 and 8 have been shown to respectively relate to characteristics of elongation, irregularity and roughness, while the remaining descriptors are calculated following an assumed regression (Mollon and Zhao, 2012). In order to generate a realistic population of non-uniform particles, a randomised set of phase angles, generated in Matlab, is included to decompose the Fourier descriptors into the elements of the Fourier spectrum which can then be used to generate a unique grain contour , such as that shown in Figure 3(b). The construction of a 3D grain by CRI of FD based contours can utilise contours generated with a constant set of descriptors, or may utilise three contours each of which is generated using divergent descriptors, to account for anisotropy effects.

It is important to note that these descriptors can be derived from the Fourier transform of the 2D grain contours which can be obtained from the analysis of grain micrographs by SEM or optical microscopy, such as that shown in Figure 3(c).

Additionally, CRI based grain generation can be carried out using fractal surface profiles as input 2D contours. These contours, such as that shown in Figure 3(a), can be generated by adjusting radii of a circle following 2D variants of Eq. 1, where θ is held constant.

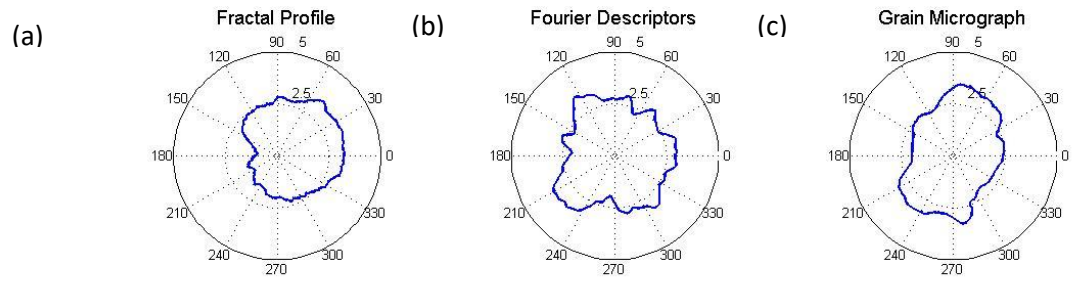

Figure 3. Sample grain contours from three sources, a simulated fractal grain profile, Fourier descriptors based contour simulation and a grain micrograph obtained by optical microscopy.

The integration of three scaled grain contours following the interpolation procedure of Mollon and Zhao results in the simulation of 3D grains such as those shown in Figure 4. This figure shows grains each of which were generated from three FD defined contours. In Figure 4(a) contours are generated from three different FD sets while in Figures 4(b) and 4(c) all three contours are generated using the same FD set. The grains thus produced exhibit irregularity typical of natural particles, however the interpolation method currently employed yields some unrealistic parallel ridges.

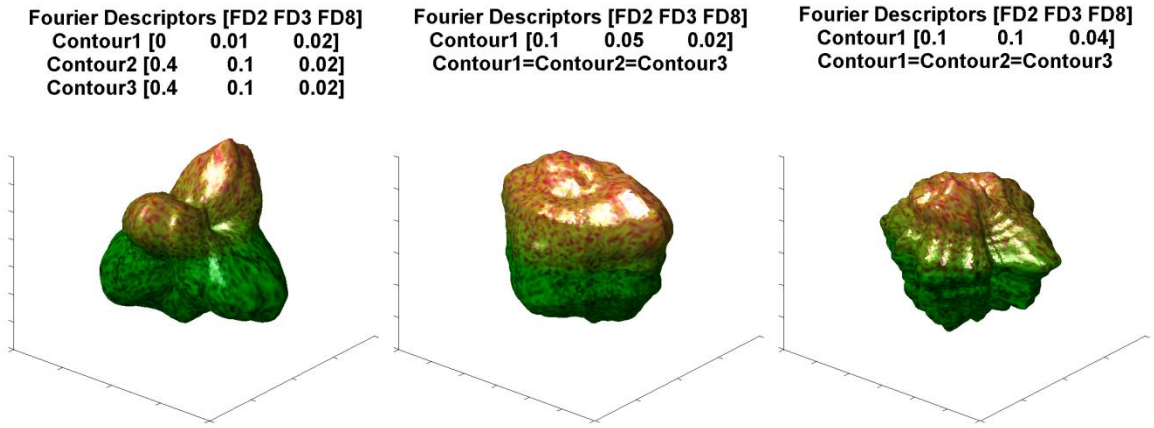

Figure 4. Sample grains simulated by the CRI method using Fourier descriptor derived contours

2.3. Method 3. Directed Polyhedra Aggregation (DPA)

Naturally occurring geomaterials occasionally exhibit morphologies that are not star-like or fully dense and thus cannot be described by a unique set of (ρ,θ,φ) coordinates. In soils, sediments, organic matter and precipitates, branching and porous forms are often encountered and the morphologies of these particles, which can be described as fractal structures are of growing interest in numerous applications (Hanaor et al., 2014). The ability to meaningfully simulate this type of particle is of value in enabling the study of the morphological dependence of hydrodynamics, mechanics, interfacial interactions and transport phenomena in granular media dominated by non star-like particles (surface points are not described by a unique set of vectors). Additionally tools for the simulation of porous and/or branching aggregates are of value for the study of particle formation in processes of aggregation, precipitation and agglomeration and the dependence of these processes on environmental conditions and system parameters (e.g. pH, temperature or surface charge).

In contrast to methods, such as FSO and CRI, that generate particles by varying the surface structure of initial primitive geodesic spheroids or Voronoi type cells, the DPA method employs an aggregation algorithm to construct particles of varied porosity and volume fractality from many convex polyhedral primary particles. Comparable algorithms for the simulation of 3D and 2D aggregates from spheroidal and cubic primary particles have been reported in earlier works (Maggi and Winterwerp, 2004, Schmid et al., 2004, Erlebacher et al., 1993).

In the presently reported DPA method the morphology of aggregate geomaterial particles was controlled using Matlab by the probability for the n-th primary particle to attach to an existing polyhedron with index i ($1 \le i \le n-1$) with respect to the history of primary particle addition, where n-1 is the existing number of primary particles. Thus, the probability that an existing particle with index $a \le i \le b$ is chosen to receive a newly placed n-th primary polyhedral particle is

$$\Pr[a \le i \le b] = \left(\frac{\varepsilon}{(n-1)^{\varepsilon}} \int_{a-1}^{b} i^{\varepsilon-1} di \right) \tag{4}$$

The *n*-th primary particle, described by face/vertex data is then added to one of the unoccupied faces of primary particle i . The probability $\Pr[a \leq i \leq b]$ is a function of the exponent ε; low exponent values result in preferential addition onto older primary particles yielding closed sphere-like aggregates, with little or no porosity (zero volume porosity is only possible when primary particles are cubic); high exponent values result in preferential addition of primary particles onto faces of recently added particles, which are likely away from the aggregated centre of mass yielding branching aggregates. This approach is readily achieved in a Matlab environment by applying the exponent ε to a uniformly distributed pseudorandom selection from existing indices.

The techniques explored here can be applied using various Platonic polyhedral elements (geometries where all faces are identical polygons) or Archimedean polyhedra (faces are of two or more types of regular polygon meeting at identical vertices) (Torquato and Jiao, 2009a). In the present work we demonstrate the application of this method using cubic and octahedral primary particles, shown respectively in Figures 5 and 6. Smoothing of sharp corners can be carried out by interpolation of the face-vertex data as illustrated for the aggregates shown in Figure 5. For the case of aggregation of octahedral primary particles, illustrated in Figure 6, in addition to the selection of a face on which to attach each new particle, the aggregation algorithm includes a step to select one of three possible rotational orientations for the newly attached octahedron. Moreover, while cubic aggregation occurs in a regular lattice, where sites are either occupied or vacant, for construction from octahedral elements, a further step is necessary to ensure that no intrusion into existing particles occurs. The simulation of fully dense aggregates is only possible with cubic elements as other Platonic or Archimedean solids do not allow fully dense spatial tiling (Torquato and Jiao, 2009b, Torquato and Jiao, 2009a). The use of octahedral or other non-cubic elements yields more porous aggregates even at high exponent values.

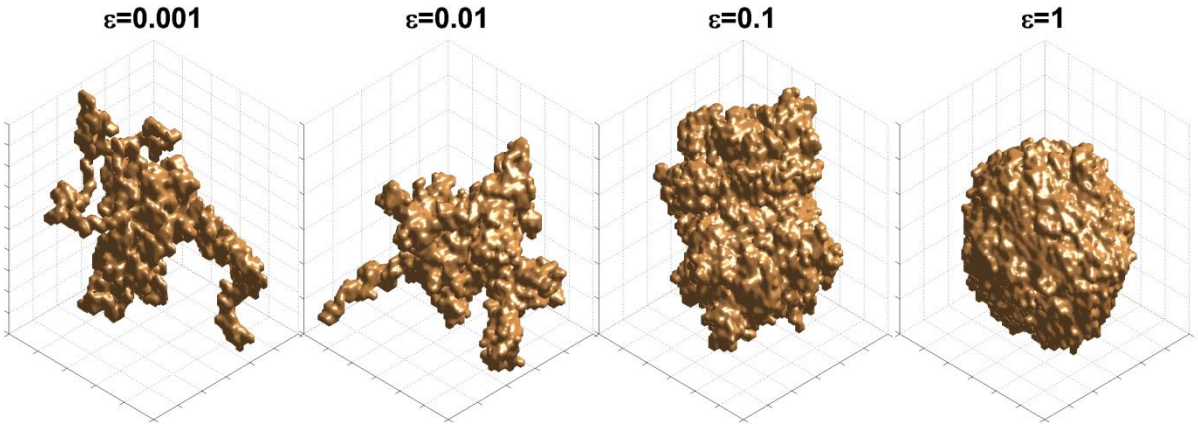

Figure 5. Grains simulated using the DPA method with cubes, showing varied values of the exponent ε resulting in particles with controllable fractality

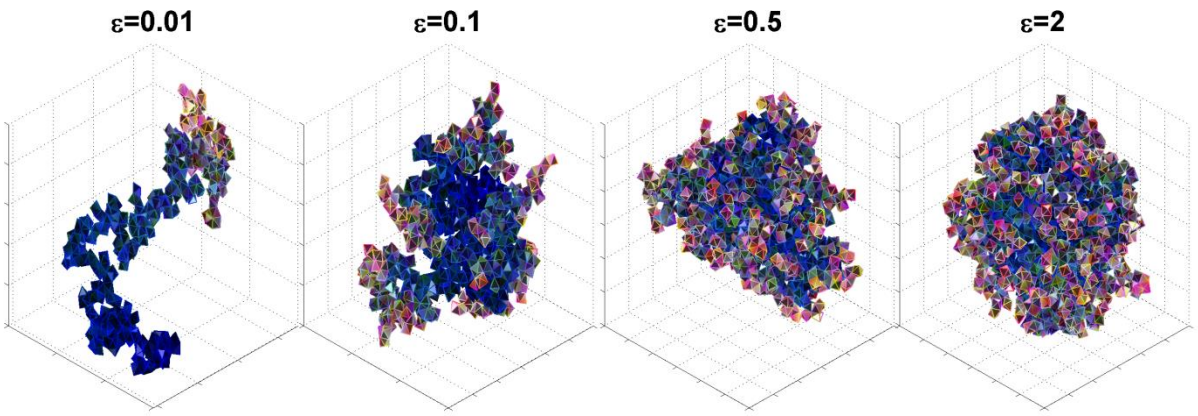

Figure 6. Grains simulated using the DPA method with octahedra, showing varied values of the exponent ε resulting in particles with controllable fractality

3. Results and Discussion

3.1. Particle simulation and fabrication

The morphologies obtained by the three methods can be fabricated using 3D printing methods and are further utilisable in DEM models. Here we show the 3D printer output from the poly-jet fabrication of particles alongside computer renderings of the morphologies.

Figure 7 shows the results of the 3D printing based fabrication of simulated grains generated by the FSO method. All features present in the simulated grain object are captured by the fabrication process employed. With less regular smaller scale features some distortion is found to occur about the grain equator for grains where the amplitude of roughness features is large relative to the grain radius. The generation of realistic surface morphologies necessitates the use of appropriate parameters of fractal dimension (D), stochastic length scale (L) and amplitude scaling (K) in the application of Eqs. 2 and 3. Simulated grains can be obtained using the FSO method with similitude to many rock and sand geomaterial particles in traditional terms of sphericity, surface roughness, convexity/concavity and elongation. However, anisotropic roughness, faceted surface regions, open pores and angular vertices are not achievable with this approach.

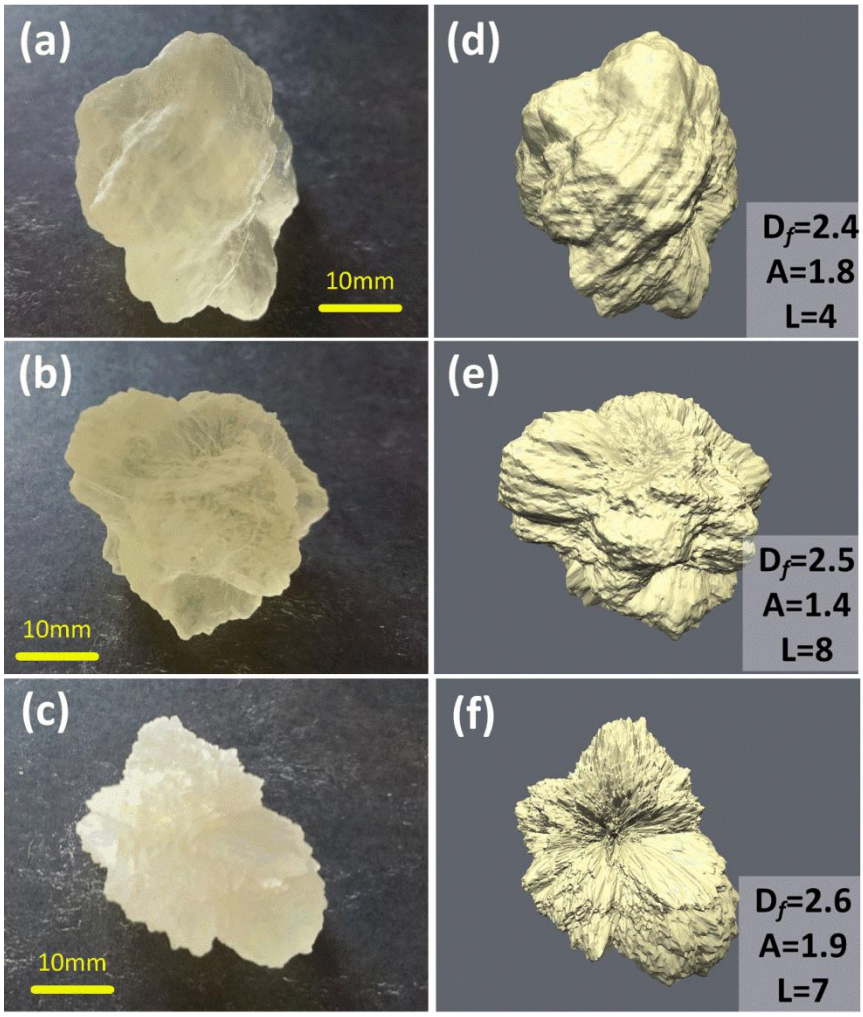

Figure 7. Comparison of printed (left) and simulated grains (right) obtained by the FSO method

Grains simulated and fabricated using the CRI approach are shown in Figure 8. Similar to previously reported results obtained from this method, grains show anisotropic features in the form of tangentially parallel surface ridges. As with the FSO method this approach shares the disadvantage of not being able to readily facilitate the generation of grains with faceted regions and/or angular vertices, frequently encountered in natural geomaterial systems. Figures 8(a) and 8(d) were generated on the basis of the mean FDs extracted from the morphological characterisation of over 1000 grains of quartz sand. Figures 8(b) and 8(e) were obtained from Garnet sand derived FDs while Figures 8(c) and (f) show the CRI generated grain on the basis of 2D contours defined by fractal surface profiles. Examination of these objects shows that the particles produced are not representative of the original material, lacking facets and angularity and further suggests that the implementation of fractal surface structure generation is more appropriately carried out using methods of the FSO type. It should be noted that more recent published studies applying random field theory on a 3D grain surface have been shown to facilitate the application of grain FDs to generate more realistic grains featuring faceted geometries without the occurrence of parallel surface ridges (Mollon and Zhao, 2014).

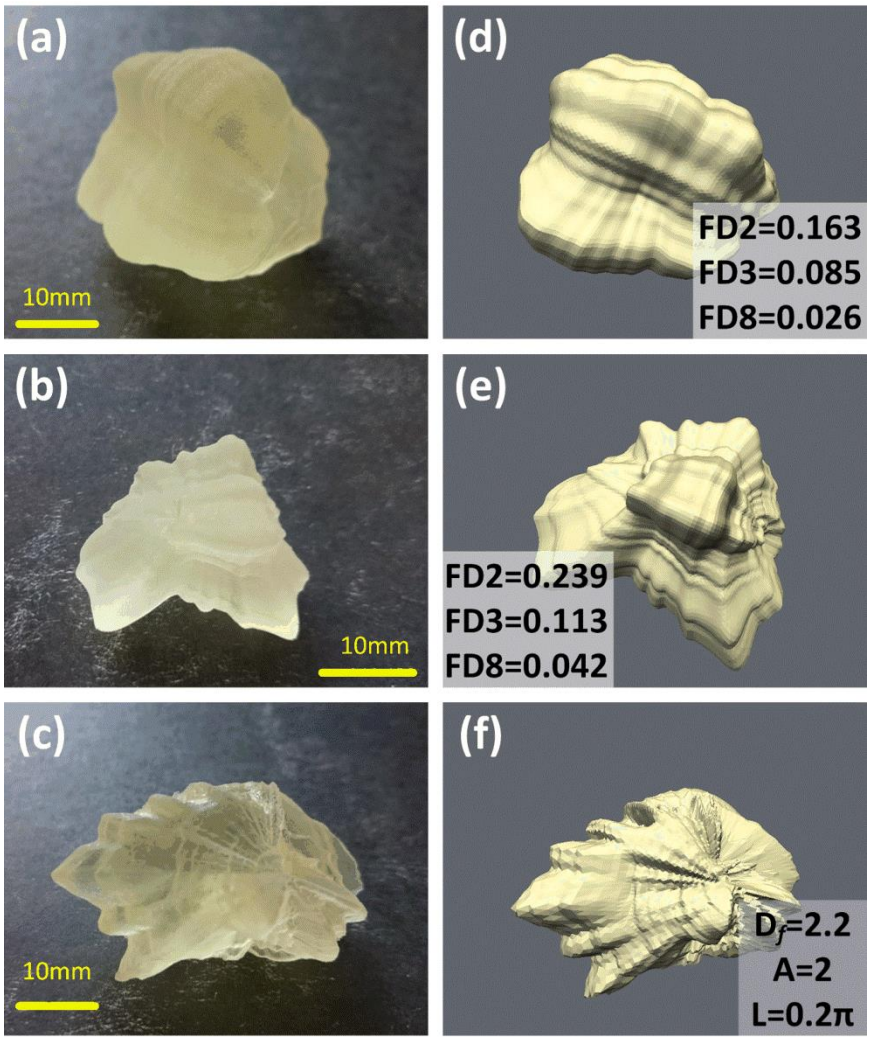

Figure 8. Comparison of printed and simulated grains obtained by the CRI method

Computer rendered and printed aggregate particles generated by the DPA methods described here are shown in Figure 9. While a wide range of realistic aggregate particles are obtainable from these methods, printed specimens exhibiting a highly branching or fractal structure are found to be fragile, particularly if a small primary particle size is employed.

The morphologies that can be generated by DPA algorithms are applicable in the study of fractal aggregates such as the type often encountered in sedimentology. By constructing a calibration curve, it is possible to control the value of the exponent ε to yield a desired aggregate fractal dimension (D_A) which corresponds to a term of the type:

$$D_A = \frac{\log V}{\log A} \tag{5}$$

where V corresponds to the true particle volume and A relates to the mean linear size of the smallest bounding box possible. The evaluation of the fractality of aggregate particles in air, soils or aqueous media and the study of the physical and mechanical behaviour of such materials in a range of applications has motivated numerous studies in recent years (Tang et al., 2003, Tang et al., 2002, Tang and Raper, 2002, Tang et al., 2001, Sorensen, 2011,

Ahmadi et al., 2011). The ability to fabricate representative particles of controlled morphology and fractal dimension can facilitate the development and implementation of new integrated experimental and computational studies into the significance of particle morphology on mechanical properties, reactivity and mobility. Moreover DPA algorithms of the type demonstrated here can be adapted to simulate and study the heterogeneous precipitation and growth of particles from solute species through chemical and biological processes (Chekroun et al., 2004, Cölfen, 2003, Hanaor et al., 2012) and also the surface chemistry dependant growth of fractal particles from suspended solid elements through processes of attraction, aggregation, cementation and sedimentation (Kranenburg, 1994, Markus et al., 2015).

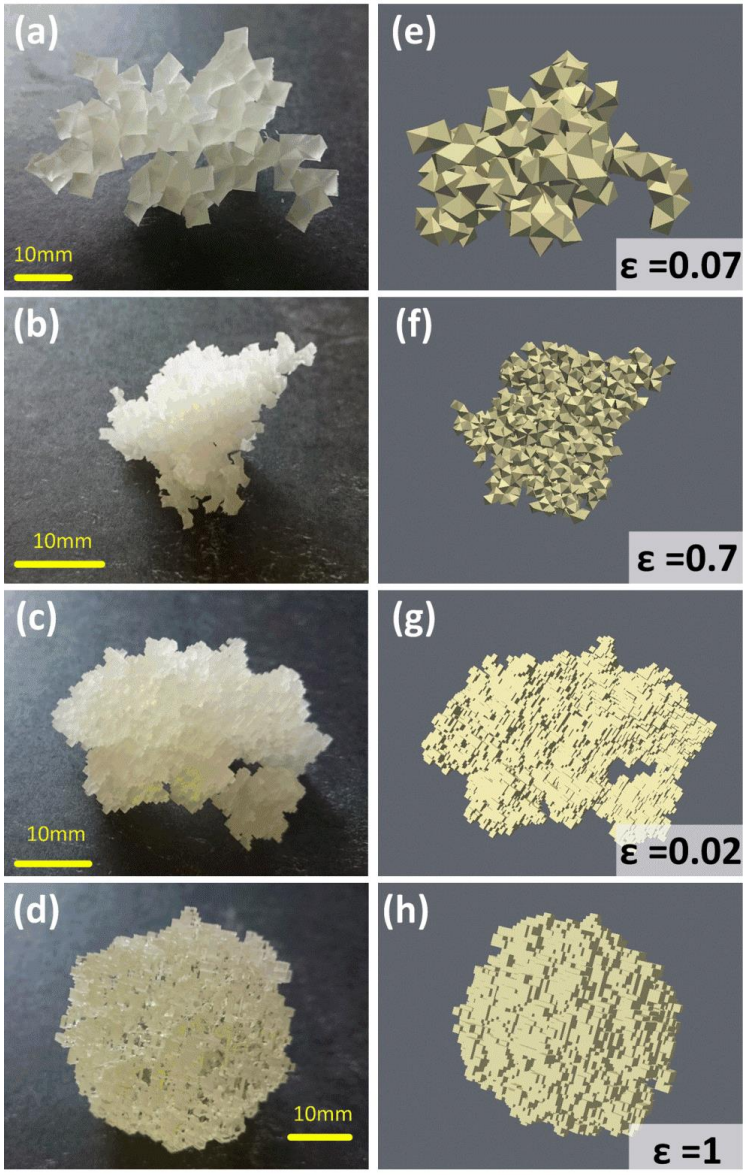

Figure 9. Comparison of printed (left) and simulated grains (right) obtained by the DPA method

3.2 Bulk material response

Grains produced by the CRI method have been subjected to geomechanical testing in a triaxial apparatus to investigate their response during compression and shear. The CRI method was chosen to produce grains for this study as it allows the input of grain parameters obtained from natural geomaterials.

Figure 10 shows a bulk print of 8,000 grains of mean diameter 2mm, which is sufficient for a triaxial specimen with dimensions of 38 mm diameter by 76 mm high. The grains are produced in one print with the same parameters so that they all have the same size but some variability in surface roughness. The process of printing and etching out this number of particles takes about 1 week. Triaxial tests have been performed using two grain shapes. These have been produced using Fourier Descriptors (0,0,0.02) referred to as rough spheres, and FDs (0.15, 0.10, 0.03) referred to as rough and angular and shown in the inset to Figure 10.

The particles were placed dry, loosely and were tamped to form the triaxial specimens, which were then subjected to a small confining stress before being saturated by percolation of water followed by back pressure saturation. The specimens were then subjected to an effective confining stress of 20 kPa before performing conventional drained shearing tests. Figure 11(a) shows the evolution of stress ratio and Figure 11(b) the associated volume strains. Values of the void ratios at the start of shearing are indicated on the figures. The results for the rough spheres demonstrate shear behaviour typical of sand. The stress ratio (q/p') of the denser specimen rises to a peak, before reducing, with associated dilation, towards an ultimate state, while the stress ratio of the looser specimen rises gradually and the specimen compresses throughout. An ultimate state with a stress ratio of about 1.5 (friction angle of 37^o) is suggested by these responses. This may be compared with an ultimate angle of about 38^o indicated by tilt table tests. Two tests are shown for the rough angular particles and in each the material compressed and the stress ratio rose steadily until the tests were terminated at large strain where the specimens were highly distorted. The second test was a repeat test using the same particles to confirm the high resistance and also to investigate whether changes in shape of the soft particles could be influencing the shear behaviour. Although a few particles were noticeably changed, it can be seen that the bulk response is not significantly affected. The friction angle implied at the test termination was 55^o. While this is unusually high, tilt table tests indicated an ultimate friction angle of 43-48^o, significantly higher than for the rough spheres and suggesting that larger strains than can be applied in the triaxial test are required for this angular material to reach an ultimate state. Although the shear responses are typical of geomaterials, during compression time dependent compressibility was observed as a result of the soft polymer comprising the grains, and further advances in material are needed to fully reproduce geomaterial properties.

Figure 10. Bulk printed granular material with inset showing rough angular particle

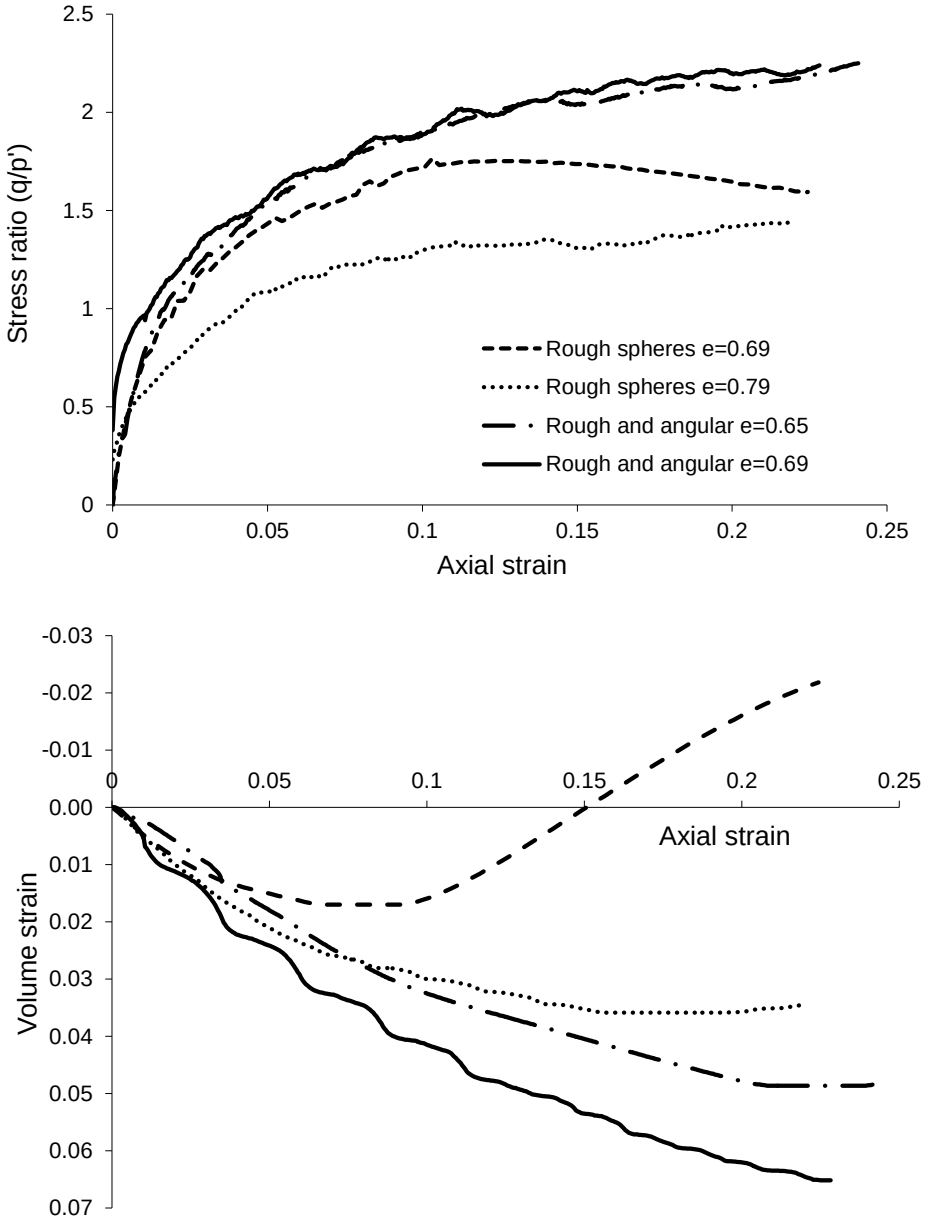

Figure 11. Triaxial shear behaviour of printed grains (a) stress ratio, axial strain and (b) volume strain, axial strain

4. Conclusions

The generation of geomaterial grain morphologies by techniques such as those described here, facilitates the fabrication of surrogate geomaterials by 3D printing. Such materials are utilisable in experimental parametric studies where morphology and material can be decoupled. Here we have focused on methods that can be applied to generate realistic and printable grain morphologies. Preliminary triaxial tests have confirmed that the printed grains are capable of reproducing aspects of shear behaviour and the significant effect that shape can have on the bulk material behaviour.

The relative advantages and drawbacks of the different grain generation methods applied here are outlined in table 2:

Table 2: Summary of grain generation methodologies investigated in the present work.

FSO:	**Superimposition of a simulated fractal surface on a 3D geodesic spheroid**	
	Benefits:	• Reproduction of natural isotropic multi-scale grain surfaces • Grain elongation control by varying highest level wavelength
	Drawbacks:	• Extraction of input parameters from real materials is challenging • Absence of smooth facets, angularity and pores • Branching morphologies cannot be simulated • Computationally intensive
CRI:	**Interpolation and morphing of three 2D contours to generate a 3D surface**	
	Benefits:	• Input parameters can be readily extracted from 2D grain data • Captures properties of elongation, roughness and irregularities • Appropriate for studying the effect of varying morphology
	Drawbacks:	• Absence of smooth facets, angularity and pores • Anisotropic features in the form of parallel ridges • Branching morphologies are not represented
DPA:	**Controlled assembly of polyhedral elements to yield branching aggregates**	
	Benefits:	• Reproduction of sediment particles and branching aggregates • Control of aggregate fractality by particle selection exponent • Input parameters can be extracted from particle characterisation
	Drawbacks:	• Surface roughness is not meaningfully represented • Cannot simulate solid monolithic particles • Computationally intensive

There are two geotechnical research directions that will significantly benefit from the ability to decouple morphology and material by means of 3D printing techniques: (i) the variation of bulk constitutive behaviour with grain morphology can be studied for constant material properties; and (ii) the variation of constitutive behaviour with material properties can be studied while maintaining constant realistic geomorphology. The first direction is restricted by printing resolution, which was 32μm in the present work, while the second direction is limited by the available range of printing materials. However, we anticipate that rapid progress in 3D printing technology in terms of printing resolution, rapidity and material versatility will address these concerns. The capabilities of ceramic-material printers is continuously increasing lending to the prediction that rather than just surrogate geomaterials, future research involving the synthesis of artificial mineral geomaterials will be made possible allowing the fabrication of standardised reference geomaterials for quality control in geotechnical testing with further potential applications as a supplementary material in construction and ground improvement.

References:

Ahmadi, A., Neyshabouri, M.-R., Rouhipour, H. & Asadi, H. (2011) Fractal dimension of soil aggregates as an index of soil erodibility. *Journal of Hydrology* **400(3)**:305-311.

Alonso-Marroquin, F. (2008) Spheropolygons: A new method to simulate conservative and dissipative interactions between 2D complex-shaped rigid bodies. *EPL (Europhysics Letters)* **83(1)**:14001.

Alonso-Marroquín, F., Mühlhaus, H. B. & Herrmann, H. J. (2008) Micromechanical investigation of granular ratcheting using a discrete model of polygonal particles. *Particuology* **6(6)**:390-403.

Alonso-Marroquín, F., Ramírez-Gómez, Á., González-Montellano, C., Balaam, N., Hanaor, D. A., Flores-Johnson, E., Gan, Y., Chen, S. & Shen, L. (2013) Experimental and numerical determination of mechanical properties of polygonal wood particles and their flow analysis in silos. *Granular Matter* **15(6)**:811-826.

Alonso-Marroquín, F. & Wang, Y. (2009) An efficient algorithm for granular dynamics simulations with complex-shaped objects. *Granular matter* **11(5)**:317-329.

Altuhafi, F., O'sullivan, C. & Cavarretta, I. (2012) Analysis of an image-based method to quantify the size and shape of sand particles. *Journal of Geotechnical and Geoenvironmental Engineering* **139(8)**:1290-1307.

Arasan, S., Akbulut, S. & Hasiloglu, A. S. (2011) The relationship between the fractal dimension and shape properties of particles. *KSCE Journal of Civil Engineering* **15(7)**:1219-1225.

Ausloos, M. & Berman, D. (1985) A multivariate Weierstrass-Mandelbrot function. *Proceedings of the Royal Society of London. A. Mathematical and Physical Sciences* **400(1819)**:331-350.

Barrett, P. (1980) The shape of rock particles, a critical review. *Sedimentology* **27(3)**:291-303.

Blott, S. J. & Pye, K. (2008) Particle shape: a review and new methods of characterization and classification. *Sedimentology* **55(1)**:31-63.

Bowman, E. T., Soga, K. & Drummond, W. (2001) Particle shape characterisation using Fourier descriptor analysis. *Geotechnique* **51(6)**:545-554.

Brisard, S., Chae, R. S., Bihannic, I., Michot, L., Guttmann, P., Thieme, J., Schneider, G., Monteiro, P. J. & Levitz, P. (2012) Morphological quantification of hierarchical geomaterials by X-ray nano-CT bridges the gap from nano to micro length scales. *American Mineralogist* **97(2-3)**:480-483.

Cavarretta, I., Coop, M. & O'sullivan, C. (2010) The influence of particle characteristics on the behaviour of coarse grained soils. *Géotechnique* **60(6)**:413-423.

Chekroun, K. B., Rodríguez-Navarro, C., González-Muñoz, M. T., Arias, J. M., Cultrone, G. & Rodríguez-Gallego, M. (2004) Precipitation and growth morphology of calcium carbonate induced by Myxococcus xanthus: implications for recognition of bacterial carbonates. *Journal of Sedimentary Research* **74(6)**:868-876.

Cho, G.-C., Dodds, J. & Santamarina, J. C. (2006) Particle shape effects on packing density, stiffness, and strength: natural and crushed sands. *Journal of Geotechnical and Geoenvironmental Engineering* **132(5)**:591-602.

Ciavarella, M., Delfine, V. & Demelio, V. (2006) A new 2D asperity model with interaction for studying the contact of multiscale rough random profiles. *Wear* **261(5)**:556-567.

Ciavarella, M., Greenwood, J. & Paggi, M. (2008) Inclusion of "interaction" in the Greenwood and Williamson contact theory. *Wear* **265(5)**:729-734.

Cölfen, H. (2003) Precipitation of carbonates: recent progress in controlled production of complex shapes. *Current opinion in colloid & interface science* **8(1)**:23-31.

Cundall, P., Drescher, A. & Strack, O. (1979) Numerical experiments on granular assemblies; measurements and observations. *Geotechnique* **29(1)**:47-65.

Ehrlich, R. & Weinberg, B. (1970) An exact method for characterization of grain shape. *Journal of sedimentary research* **40(1)**.

Erlebacher, J., Searson, P. & Sieradzki, K. (1993) Computer simulations of dense-branching patterns. *Physical Review Letters* **71(20)**:3311.

Fraysse, N., Thomé, H. & Petit, L. (1999) Humidity effects on the stability of a sandpile. *The European Physical Journal B-Condensed Matter and Complex Systems* **11(4)**:615-619.

Hanaor, D., Chironi, I., Karatchevtseva, I., Triani, G. & Sorrell, C. (2012) Single and mixed phase TiO_2 powders prepared by excess hydrolysis of titanium alkoxide. *Advances in Applied Ceramics* **111(3)**:149-158.

Hanaor, D. A., Gan, Y. & Einav, I. (2013) Effects of surface structure deformation on static friction at fractal interfaces. *Geotechnique Letters* **3(2)**:52-58.

Hanaor, D. A., Gan, Y. & Einav, I. (2015) Contact mechanics of fractal surfaces by spline assisted discretization. *International Journal of Solids and Structures* **59**:121-131.

Hanaor, D. a. H., Ghadiri, M., Chrzanowski, W. & Gan, Y. (2014) Scalable surface area characterisation by electrokinetic analysis of complex anion adsorption. *Langmuir* **30(50)**:15143-15152.

Komvopoulos, K. (2008) Effects of multi-scale roughness and frictional heating on solid body contact deformation. *Comptes Rendus Mécanique* **336(1)**:149-162.

Kranenburg, C. (1994) The fractal structure of cohesive sediment aggregates. *Estuarine, Coastal and Shelf Science* **39(6)**:451-460.

Krumbein, W. C. & Sloss, L. L. (1951) Stratigraphy and sedimentation. *Soil Science* **71(5)**:401.

Langston, P., Ai, J. & Yu, H.-S. (2013) Simple shear in 3D DEM polyhedral particles and in a simplified 2D continuum model. *Granular Matter* **15(5)**:595-606.

Liao, C.-W., Yu, J.-H. & Tarng, Y.-S. (2010) On-line full scan inspection of particle size and shape using digital image processing. *Particuology* **8(3)**:286-292.

Maggi, F. & Winterwerp, J. (2004) Method for computing the three-dimensional capacity dimension from two-dimensional projections of fractal aggregates. *Physical Review E* **69(1)**:011405.

Markus, A., Parsons, J., Roex, E., De Voogt, P. & Laane, R. (2015) Modeling aggregation and sedimentation of nanoparticles in the aquatic environment. *Science of the Total Environment* **506**:323-329.

Matsushima, T., Saomoto, H., Matsumoto, M., Toda, K. & Yamada, Y. (2014) Discrete element simulation of an assembly of irregularly-shaped grains: Quantitative comparison with experiments. *Springer-Verlag, Heidelberg.* **44(2)**.

Miskin, M. Z. & Jaeger, H. M. (2013) Adapting granular materials through artificial evolution. *Nature Materials* **12(4)**:326-331.

Mollon, G. & Zhao, J. (2012) Fourier–Voronoi-based generation of realistic samples for discrete modelling of granular materials. *Granular Matter* **14(5)**:621-638.

Mollon, G. & Zhao, J. (2013a) Generating realistic 3D sand particles using Fourier descriptors. *Granular Matter* **15(1)**:95-108.

Mollon, G. & Zhao, J. (2013b) The influence of particle shape on granular Hopper flow. *Powders and Grains*:690-693.

Mollon, G. & Zhao, J. (2014) 3D generation of realistic granular samples based on random fields theory and Fourier shape descriptors. *Computer Methods in Applied Mechanics and Engineering*.

Natalini, P., Patrizi, R. & Ricci, P. E. (2008) The Dirichlet problem for the Laplace equation in a starlike domain of a Riemann surface. *Numerical Algorithms* **49(1-4)**:299-313.

Pena, A., Garcia-Rojo, R. & Herrmann, H. (2007) Influence of particle shape on sheared dense granular media. *Granular Matter* **9(3-4)**:279-291.

Persson, A.-S. & Frenning, G. (2012) An experimental evaluation of the accuracy to simulate granule bed compression using the discrete element method. *Powder Technology* **219**:249-256.

Pourghahramani, P. & Forssberg, E. (2005) Review of applied particle shape descriptors and produced particle shapes in grinding environments. Part I: Particle shape descriptors. *Mineral Processing & Extractive Metall. Rev.* **26(2)**:145-166.

Qin, J., Zhong, D., Wang, G. & Ng, S. L. (2013) Influence of particle shape on surface roughness: Dissimilar morphological structures formed by man-made and natural gravels. *Geomorphology* **190**:16-26.

Robertson, M. (1936) Analytic functions star-like in one direction. *American Journal of Mathematics*:465-472.

Russel, A. (2014) How water retention in fractal soils depends on particle and pore sizes, shapes, volumes and surface areas. *Géotechnique* **64(5)**:379-390.

Salot, C., Gotteland, P. & Villard, P. (2009) Influence of relative density on granular materials behavior: DEM simulations of triaxial tests. *Granular matter* **11(4)**:221-236.

Scheel, M., Seemann, R., Brinkmann, M., Di Michiel, M., Sheppard, A., Breidenbach, B. & Herminghaus, S. (2008) Morphological clues to wet granular pile stability. *Nature Materials* **7(3)**:189-193.

Schmid, H.-J., Tejwani, S., Artelt, C. & Peukert, W. (2004) Monte Carlo simulation of aggregate morphology for simultaneous coagulation and sintering. *Journal of Nanoparticle Research* **6(6)**:613-626.

Sorensen, C. (2011) The mobility of fractal aggregates: a review. *Aerosol Science and Technology* **45(7)**:765-779.

Tang, P., Chew, N. Y., Chan, H.-K. & Raper, J. A. (2003) Limitation of determination of surface fractal dimension using N2 adsorption isotherms and modified Frenkel-Halsey-Hill theory. *Langmuir* **19(7)**:2632-2638.

Tang, P., Greenwood, J. & Raper, J. A. (2002) A model to describe the settling behavior of fractal aggregates. *Journal of Colloid and Interface Science* **247(1)**:210-219.

Tang, P. & Raper, J. A. (2002) Modelling the settling behaviour of fractal aggregates–a review. *Powder Technology* **123(2)**:114-125.

Tang, S., Ma, Y. & Shiu, C. (2001) Modelling the mechanical strength of fractal aggregates. *Colloids and surfaces A: Physicochemical and engineering aspects* **180(1)**:7-16.

Tarnawski, V. R., Momose, T., Leong, W., Bovesecchi, G. & Coppa, P. (2009) Thermal conductivity of standard sands. Part I. Dry-state conditions. *International Journal of Thermophysics* **30(3)**:949-968.

Thomas, M., Wiltshire, R. & Williams, A. (1995) The use of Fourier descriptors in the classification of particle shape. *Sedimentology* **42(4)**:635-645.

Thomas, P. A. & Bray, J. D. (1999) Capturing nonspherical shape of granular media with disk clusters. *Journal of Geotechnical and Geoenvironmental Engineering* **125(3)**:169-178.

Torquato, S. & Jiao, Y. (2009a) Dense packings of polyhedra: Platonic and Archimedean solids. *Physical Review E* **80(4)**:041104.

Torquato, S. & Jiao, Y. (2009b) Dense packings of the Platonic and Archimedean solids. *Nature* **460(7257)**:876-879.

Yan, W. & Komvopoulos, K. (1998) Contact analysis of elastic-plastic fractal surfaces. *Journal of Applied Physics* **84(7)**:3617-3624.